RESEARCH ON THE DESIGN AND OPTIMIZATION OF TOMATO TRANSPLANTING CLAWS BASED ON SUPERELASTIC MATERIAL
/
基于超弹性材料的番茄移栽机械手设计与优化研究

Dong JI[1)], Qingyu MENG[1)], Jiaqi LI[1)], Jia SHI[1)], Zhao ZHU[1)], Haibo JIAO[1)], Shengbin MA[1)], Subo TIAN[2)], Fengbo LIU*[1)]

[1)] Liaoning Agricultural Vocational and Technical College, 76 Yucai Road, Yingkou 115009, China;
[2)] College of Engineering, Shenyang Agricultural University, 120 Dongling Road, Shenyang 110866, China
Tel: 17741575562; E-mail: 13325259481@163.com
Corresponding author: Fengbo LIU
DOI: https://doi.org/10.35633/inmateh-78-77

Keywords: *transplanting claw; superelastic material; automatic seedling feeding; NSGA-II algorithm; optimization design;*

ABSTRACT
Currently, transplanting claws may cause damage to seedling stems or roots during the seedling extraction process. In this study, a dynamic simulation model of the seedling extraction process using transplanting claws was established and analyzed. Foam thickness and width along with the clamping torque were selected as experimental factors, while stem stress and deformation were used as evaluation indicators in a Box–Behnken response surface design. Based on variance analysis of the regression model, the significance of each factor and their interactions was determined, and corresponding regression equations were established. Subsequently, a multi-objective optimization of the regression models was performed using the NSGA-II algorithm, and optimal solutions were identified based on the Pareto frontier. The results show that the optimal parameter combination is obtained at a foam thickness of 6 mm, a foam width of 6.4 mm, and a clamping torque of 0.4 N·m. Under these conditions, the stem stress is 3.1893 MPa and the deformation is 0.8024 mm, which are in close agreement with the predicted values. These findings demonstrate that the combination of the NSGA-II algorithm and the Box–Behnken response surface method is effective for optimizing transplanting claw parameters. However, as this study is based solely on simulation, experimental validation using actual tomato seedlings is required before practical application, which will be addressed in future work.

摘要
目前，移栽爪取苗过程中容易对茎秆或苗坨造成损伤。本文通过建立移栽爪取苗过程动力学仿真模型并且进行仿真分析。以泡棉厚度、宽度、夹持扭矩为试验因素，以取苗成功后番茄茎秆被夹持处所受应力与形变量为试验指标进行 Box-Behnken 组合试验。根据回归模型的方差分析，确定各试验因素及其交互作用的显著性，建立试验指标对应的回归方程。基于 NSGA-Ⅱ算法对回归方程进行多目标优化，求解优化目标的帕累托（Pareto）前沿图。当泡棉厚度为 6mm，泡棉宽度为 6.4mm，夹持扭矩为 0.4N·m 时为最优解，茎秆所受应力为 3.1893MPa、形变量为 0.8024mm，与预测值接近，证明 NSGA-Ⅱ结合响应面法在移栽爪优化的可行性。但由于本研究完全基于仿真，实际应用前仍需在真实番茄幼苗上进行实验验证，这将在未来工作中开展。

INTRODUCTION
As a key executive component of vegetable transplanters, the transplanting claw performs the operational processes of seedling picking, conveying and transplanting. Its structural design and operational accuracy determine the transplanting success rate of the transplanter, and it is the core of realizing the mechanization and automation of vegetable seedling transplanting *(Choi et al., 2002; Jo et al., 2018; Sharma et al., 2022)*. During transplanting operations, the transplanting claw must adapt to the morphological characteristics of plug seedlings, and achieve accurate seedling picking, stable conveying and non-damaging transplanting under high-speed operation *(Chen et al., 2015)*. This imposes stringent requirements on its structural rigidity and the regulation of clamping force *(Cui et al., 2017)*.

Nowadays, with the development of mechanized vegetable transplanting, the development of transplanting claw have remained a crucial direction for enhancing the performance of transplanter. In the early stage of transplanter research, advanced agricultural countries such as Europe, America, Japan and South Korea took the structural optimization of transplanting claws as key research contents.

By integrating mechanical design with mechatronic control technology, they have developed transplanting claw structures adapted to different crops, which has laid a foundation for the high-speed and automated development of transplanters *(Jia et al., 2019)*. With the increasing demand for mechanized vegetable transplanting in China, the transplanting claws have also been progressively advanced.

However, there is still a gap between domestic transplanting claws and the international advanced level in terms of operational accuracy, universality and adaptability. It has become the key factor restricting the development of the automatic transplanters in China *(Wen et al., 2021; Wang et al., 2025)*.

At present, transplanting claws are classified into some types which are clamping transplanting claw, ejecting transplanting claw and grabbing transplanting claw. Transplanting claws with different structures have their respective advantages and disadvantages in operational performance. The clamping transplanting claw has become the most widely used type in existing transplanters due to its advantages of simple structure and convenient control. But the clamping force is difficult to regulate precisely, which is prone to cause damage to seedling stem. The ejecting transplanting claw can effectively reduce the seedling damage rate, but it has high requirements for the positioning accuracy of plug trays. The grabbing transplanting claw features strong universality, but it exists problems such as complex structure and low operational efficiency (*Paradkar et al., 2021*). In the case of high-speed transplanting operations, traditional transplanting claws also have problems such as insufficient matching between the motion trajectory and the seedling picking (*Cheng et al., 2021*). Therefore, it could exist problems such as complex structure and low operational efficiency.

In recent years, scholars have conducted extensive research on the structural optimization, kinematic simulation and performance testing of transplanting claws. Some studies have optimized the motion trajectory of the transplanting claws by improving core transmission components such as linkage mechanisms and cam mechanisms. The aim is to enhance the accuracy of seedling extraction and planting (*Wang et al., 2020*). Other studies have developed modular transplanting claw which can adjust spacing and clamping range to meet the adaptation requirements for multiple types of vegetable seedlings, and it will improve the versatility (*Xin et al., 2023*). Some scholars have combined machine vision technology to achieve non-destructive monitoring and precise positioning of the seedling extraction process during transplantation (*Yin et al., 2010; He et al., 2023*). However, the existing research results still have many shortcomings. Some high-precision transplanting claws rely on imported core components, which are costly and difficult to be promoted locally (*Mohith et al., 2019; Francesca et al., 2019*). During the process of transplanting seedlings with transplanting claws, the problem of damaging the seedlings often occurs (*Chang et al. 2023; Kunz et al., 2018*).

The performance optimization and innovative design of the transplanting claw are crucial for improving the operation quality of vegetable transplanting and promoting the automation development of transplanter (*Khadatkar et al., 2024; Daisuke et al., 2019*). In this study, based on the physical characteristics of vegetable seedlings, the practical requirements of transplanting operations, and the structural configurations, a clamping transplanting claw based on superelastic materials was developed. This design provides a theoretical basis and research insights for the structural innovation, performance optimization, and universal design of transplanting claws.

MATERIALS AND METHODS

Transplanting claw design

As a critical component of the transplanter, the seedling extraction success rate of the transplanting claw serves as a key indicator for evaluating overall transplanting performance. The common structures of transplanting claws can be categorized into two types: clamping-type and pin-type mechanisms. Given the relatively thick and robust stems of tomato seedlings, a clamping-type transplanting claw constructed from superelastic materials was developed. Compared with leafy vegetable seedlings, tomato plants possess sturdier stems, making clamping operations simpler and more efficient.

Superelastic materials, such as rubber, sponge, foam, and silicone, exhibit favorable mechanical properties, including flexibility and recoverability. They are widely used in daily life and industrial applications. In this design, superelastic EPE foam is employed as the contact material between the clamping-type transplanting claw and the substrate–stem system. By utilizing the advantageous mechanical properties of superelastic materials, efficient and low-damage seedling extraction can be achieved.

When the transplanting claw closed, the two clamping plates remain parallel. Each plate consists of a steel clamping sheet and an EPE foam layer, which together secured the tomato seedling stem and ensured that the stems were not destroyed. When the transplanting claw opened, the distance between the tips of the two plates matched the width of a single cell in the seedling tray.

This ensured that the tomato seedling stem remains positioned between the plates throughout the entire grasping process. The design is illustrated in Figure 1.

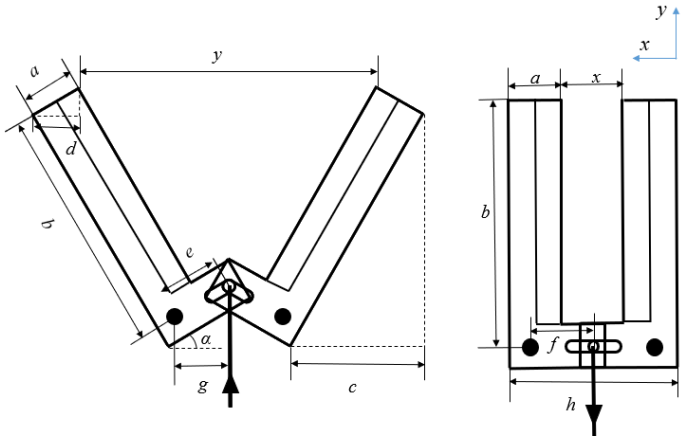

Fig. 1 - The Design of transplanting claw
(a) Claws opened *(b) Claw closed*

The transplanting claw was driven by a cylinder, whose extension and retraction controlled the opening and closing of the clamping plates. The outer side of each clamping plate was reinforced with a steel sheet of specified thickness, while the inner side was lined with EPE foam. When the cylinder extends, the clamping plates open to a defined angle, forming the open state of the transplanting claw. The distance between the two plates corresponds to the width of a single cell in the seedling tray. When the cylinder retracts, the plates become parallel, corresponding to the grasping state, and grasp the seedlings.

When the transplanting claw is opened, the calculation formula is as follows.

$$d+\frac{y}{2}=b\cdot\sin\alpha+\left(e+\frac{h-2\cdot g}{2}\right)\cdot\cos\alpha \tag{1}$$

$$\cos\alpha=\frac{d}{a}=\frac{h-2\cdot g}{2\cdot e} \tag{2}$$

$$\sin\alpha=\frac{c}{b} \tag{3}$$

When the transplanting claw is closed, the calculation formula is as follows.

$$2a+x+2g=2f+h \tag{4}$$

Summarizing these formulas, it can be obtained.

$$(2g-h)x+2eg+4eg+2hg+2he-4g^2=2b\sqrt{2e^2-(h-2g)^2} \tag{5}$$

$$a+\frac{x}{2}-\frac{h-2\cdot g}{2}=f \tag{6}$$

In the equation: a is the thickness of the clamping plate, mm; b is the length of the clamping plate, mm; c is the projection of the claw length onto the x-axis when the transplanting claw is open, mm; d is the projection of the clamping plate thickness onto the x-axis when the transplanting claw is open, mm; e is the distance between the hinge point of the clamping plate and the inner edge center of the slot when the transplanting claw is open, mm; f is the distance between the hinge point of the clamping plate and the outer edge center of the slot when the transplanting claw is closed, mm; g is the horizontal distance between the hinge point and the slot when the transplanting claw is open, mm; h is the width between the lower edges of the two clamping plates when the transplanting claw is closed, mm; x is the opening width between the two clamping plates when the transplanting claw is closed, mm; y is the opening width between the two clamping plates when the transplanting claw is open, mm; α is the angle between the clamping plate and the x-axis when the transplanting claw is open.

Substituting the known parameters into the above formula, the design parameters of the transplanting claw can be obtained, as shown in Table 1.

Table 1

Transplanting claw parameter

Parameter	Value	Unit	Parameter	Value	Unit
a	14	mm	*g*	9	mm
b	64	mm	*h*	31	mm
c	22	mm	*x*	3	mm
d	13	mm	*y*	43	mm
e	6	mm	*α*	20	°
f	9	mm			

The structure of the transplanting claw is shown in Figure 2.

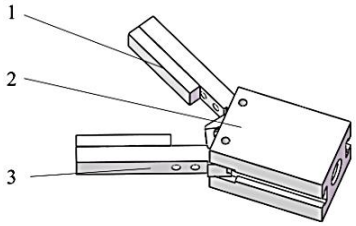

Fig. 2 - Transplanting claw structure

1. EPE foam; 2. Transplanting claw cylinder; 3. Steel plate

Construction of the simulation model for the transplanting claw

The seedling taking process begins when the transplanting claw closes and makes contact with the tomato seedling stem. As the EPE foam contacts the stem, the pair of clamping plates gradually tighten, causing the foam to undergo substantial deformation and wrap around the tomato stem. The transplanting claw then moves upward, relying on the friction between the foam and the stem to extract the seedling plug from the tray. The seedling stem undergoes deformation while being clamped by the plates. Excessive deformation can compress the stem, resulting in mechanical damage and subsequently reducing the survival rate. Therefore, the deformation and stress experienced by the tomato seedling stem are used as evaluation criteria.

The foam thickness, foam width, and clamping force of the clamping-type transplanting claw have the greatest influence on the tomato seedling stem during the seedling taking process. If the foam layer is too thin, excessive deformation of the stem may occur, which can damage its internal structure. A foam layer which is too narrow may result in failure to take the seedling. An insufficient clamping force reduces the success rate of seedling taking, whereas an excessively high force may cause stem damage. Therefore, these parameters are considered key factors in optimizing the clamping-type transplanting claw. Simulation experiments are employed to determine the optimal design parameters.

(1) Establishment and simplification of the seedling plug model

The seedling plug model consists of the substrate block, tomato leaves, and tomato stem. However, during the transplanting process, the transplanting claw does not contact the tomato leaves, and the interactions among leaves of adjacent seedlings are negligible. Therefore, the leaf structure is simplified when constructing the three-dimensional seedling plug model. The material parameters used for constructing the seedling plug model are listed in Tables 2 and 3.

Table 2

Parameters of the substrate block

Parameter	Elastic modulus (G) / MPa	Poisson's ratio (μ)	Density (ρ) / g·mm³
Value	28	0.4	7.5×10^{-1}

Table 3

Simulation parameters of the tomato seedling stem

Parameter	Value	Unit	Parameter	Value	Unit
Elastic modulus (E_x)	21.3	MPa	Poisson's ratio (μ_{yz})	0.34	
Elastic modulus (E_y)	21.3	MPa	Poisson's ratio (μ_{xz})	0.34	
Elastic modulus (E_z)	6.08	MPa	Shear modulus (G_{xy})	7.95	MPa

Parameter	Value	Unit	Parameter	Value	Unit
Density (ρ)	6×10^{-1}	g/mm^3	Shear modulus (G_{xz})	2.94	MPa
Poisson's ratio (μ_{xy})	0.034		Shear modulus (G_{yz})	2.94	MPa

(2) Simplification and processing of the transplanting claw model

Based on the previously designed 3D model of the transplanting claw, the model was simplified by removing the connecting pins at each joint and eliminating all bolt connections. The frame of the transplanting claw was treated as a rigid body, whereas the clamping plates and the attached EPE foam were defined as flexible bodies. A rigid-flexible coupling approach was adopted to simulate the seedling taking process and improve computational efficiency. The material parameters of structural steel and EPE foam are listed in Table 4.

Table 4

Material parameters

Material	Simulation parameters		
	Elastic modulus (G) / MPa	Poisson's ratio (μ)	Density (ρ) / g·mm^{-3}
Structural steel	2.1×10^5	0.25	7.85
EPE foam	3	0.01	2.9×10^{-2}

(3) Importing the simulation model

According to Saint-Venant's principle, the model cannot be segmented along the clamping edges, as such treatment would lead to stress concentration at the clamping region during simulation and result in inaccurate calculations. Therefore, the tomato stem was extended by 10 mm at both ends before performing the solid segmentation. Since the seedling extraction position is approximately 25–35 mm above the stem base, the clamping region of the stem was specifically segmented to allow clear observation of deformation at the clamping site. This segmentation provides essential deformation data for the subsequent optimization of the transplanting claw.

The completed three-dimensional model was imported into the Transient Structural module of ANSYS Workbench. The segmented stem components were merged through common-node processing to ensure proper continuity within the simulation.

(4) Preprocessing of the simulation model

Based on the material properties listed above for each model component, a planar surface was added beneath the substrate block and defined as the ground. This plane was set as a fixed support. The bottom of the substrate block was placed in contact with the ground plane, and the interface was defined as frictionless. A weak spring control was applied to prevent unintended movement of the seedling plug during simulation. The seedling extraction process involves geometric nonlinearity, as the foam pad of the transplanting claw changes its contact state with the tomato stem. Both contact pressure and contact area vary throughout the process; therefore, the large-deformation option was enabled. Based on experimental results, the average extraction force of the seedling plug was measured as F = 5.71 N. A downward pulling force of the same magnitude was applied to the plug, followed by mesh generation for the model. The ground surface was defined as a rigid body. To improve computational accuracy, body-sizing control was applied during meshing. A tetrahedral mesh was primarily used, with a mesh size of 1.0 mm assigned to the stem and foam regions and 2 mm for the remaining components. The resulting mesh model is shown in Figure 3.

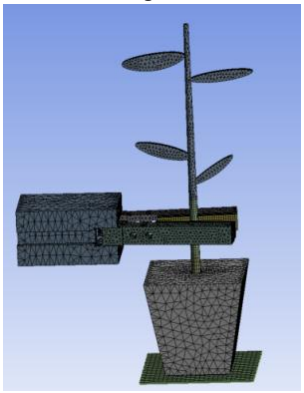

Fig. 3 - Mesh division of the simulation model

(5) Simulation setting

According to the design parameters of the transplanter, the kinematic pairs, contact types, and friction coefficients between individual components were defined. The clamping duration of the transplanting claw was set to 0.5 s, followed by the extraction of the seedling from the tray, which was assigned a duration of 1 s. Thus, the total simulation time was 1.5 s. The large-deformation option was enabled, and the time step was set to 0.001 s. Each test condition was simulated twice, with 20 CPU cores assigned for computation.

Simulation experiments of seedling taking using the transplanting claw

(1) Box–Behnken simulation experiment design

Based on the above analysis of the seedling extraction process, the foam thickness, foam width, and clamping force of the transplanting claw have the greatest influence on the mechanical response of the tomato stem and the overall success of seedling taking. In the simulation experiment design, these three variables were selected as the experimental factors (m = 3). The evaluation indices were the stress (y_1) and deformation (y_2) at the clamping region of the stem. A simulation experiment was designed accordingly, as shown in Table 5.

Table 5

Factor level coding table

Level	Factor		
	Foam thickness (x_1) / mm	Foam width (x_2) / mm	Clamping torque (x_3) / N·m
-1	3	4	0.4
0	4.5	7	0.6
1	6	10	0.8

Preliminary single-factor simulations revealed that a foam thickness below 3 mm caused excessive stem deformation (greater than 1.5 mm), while a thickness above 6 mm provided no additional benefit. A foam width below 4 mm led to seedling slip, whereas a width above 10 mm interfered with adjacent cells. Regarding clamping torque, a value below 0.4 N·m resulted in incomplete clamping, while a value above 0.8 N·m caused visible stem indentation.

(2) Simulation results

Using the Transient Structural module of ANSYS Workbench, the entire seedling extraction process was simulated. Based on the design parameters listed in Table 4-5, a total of 17 simulation runs were conducted. The simulation results are summarized in Table 6.

Table 6

Experimental design and simulation results

No.	x_1	x_2	x_3	y_1	y_2
1	4.5	7	0.6	4.9621	1.2347
2	6	4	0.6	5.8268	1.6642
3	3	10	0.6	3.3795	1.2387
4	4.5	7	0.6	4.9621	1.2347
5	6	7	0.4	4.5927	0.7796
6	4.5	7	0.6	4.9621	1.2347
7	4.5	7	0.6	4.9621	1.2347
8	3	7	0.4	3.6185	0.8764
9	3	4	0.6	3.1864	1.5893
10	4.5	4	0.4	4.9589	0.8968
11	4.5	10	0.8	5.7748	1.1784
12	6	7	0.8	5.7934	1.8025
13	4.5	7	0.6	4.9621	1.2347

No.	x_1	x_2	x_3	y_1	y_2
14	6	10	0.6	3.1721	1.3754
15	4.5	4	0.8	5.9861	1.7894
16	4.5	10	0.4	3.2786	0.9856
17	3	7	0.8	5.3106	0.9963

(3) Transient dynamics simulation results and analysis

The simulation results are shown in Figure 4. The animation indicates that during the first 0.5 s, the transplanting claw clamps the tomato stem, and between 0.5 and 1.5 s, the claw maintains its grip and successfully extracts the seedling from the tray. One case at the 1.5 second is shown in the figure 4, during the clamping and extraction of the seedling stem, the pulling force leads to significant stress concentrations at the base of the claw, particularly near the connection between the claw mechanism and the cylinder.

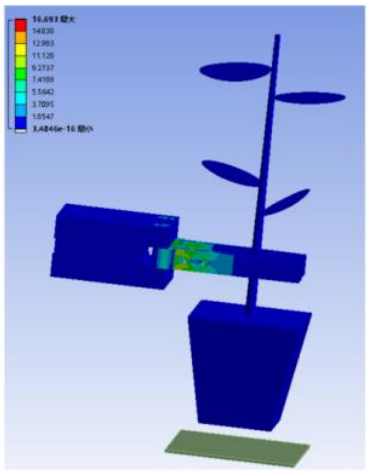

Fig. 4 - Case of stem clamping at 1.5 s

Since the tomato stem material was segmented in the preprocessing step, the stress distribution at the clamping region can be independently examined. One case is shown in Figure 5 (stress nephogram). As observed, the stress on the stem is primarily concentrated at the contact interface between the foam pad and the tomato stem, which is consistent with the actual stress pattern during clamping. This indicates that the simulation results are reasonable and reliable.

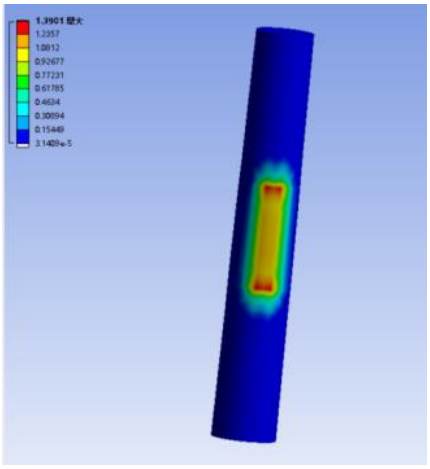

Fig. 5 - Stress distribution at the clamping region of the tomato stem

The cross-sectional stress contour was extracted to examine the detailed stress distribution at the clamping section of the tomato stem. One case is shown in Figure 6 (stress nephogram). Examination of the internal stress distribution reveals a distinct stress band extending from both sides of the clamping position toward the center of the stem cross-section. Within this stress band, the clamped region exhibits noticeably higher stress, whereas the non-clamped regions show relatively low stress. The computed results align well with the actual stress pattern experienced by the stem during clamping.

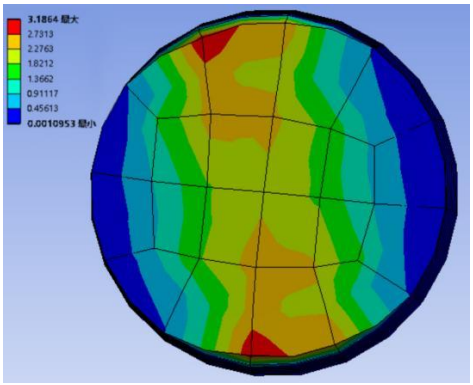

Fig. 6 - Stress distribution on the cross-section of the clamped tomato stem.

RESULTS

Quadratic regression combined test

Based on the simulation design and results, the data were processed using Design-Expert software to perform an analysis of variance (ANOVA). The ANOVA results for the effects of the design parameters of the clamping-type transplanting claw on stem stress and deformation are presented in Tables 7 and 8.

Table 7

Analysis of variance of stress on tomato stem

Source	Sum of squares	Degrees of freedom	Mean square	F-value	P-value
Polynomial terms	15.42	9	1.71	57.26	<0.0001**
X_1	1.89	1	1.89	63.23	<0.0001**
X_2	2.37	1	2.37	79.19	<0.0001**
X_3	5.15	1	5.15	172.03	<0.0001**
X_1X_2	2.03	1	2.03	67.78	<0.0001**
X_1X_3	0.0604	1	0.0604	2.02	0.1984
X_2X_3	0.5395	1	0.5395	18.04	0.0038**
X_1^2	1.62	1	1.62	54.26	0.0002**
X_2^2	0.8528	1	0.8528	28.51	0.0011**
X_3^2	1	1	1	33.46	0.0007**
Residual	0.2094	7	0.0299		
Lack of fit	0.2094	3	0.0698		
Pure error	0	4	0		
Total	15.63	16			

Note: **Highly significant level ($p < 0.01$); *Significant level ($p < 0.05$).

The significance of the regression model was evaluated at the α=0.05 significance level. According to the ANOVA results, the regression model for the stress on the tomato stem exhibits a P-value less than 0.0001, indicating that the model is statistically significant.

Table 8

Analysis of variance of deformation of tomato stem

Source	Sum of squares	Degrees of freedom	Mean square	F-value	P-value
Polynomial terms	1.49	9	0.1657	35.04	<0.0001**
X_1	0.106	1	0.106	22.42	0.0021**
X_2	0.1687	1	0.1687	35.66	0.0006**
X_3	0.6206	1	0.6206	131.23	<0.0001**
X_1X_2	0.001	1	0.001	0.2019	0.6668
X_1X_3	0.2039	1	0.2039	43.1	0.0003**
X_2X_3	0.1224	1	0.1224	25.89	0.0014**
X_1^2	0.0187	1	0.0187	3.96	0.087

Source	Sum of squares	Degrees of freedom	Mean square	F-value	P-value
X_2^2	0.1154	1	0.1154	24.39	0.0017**
X_3^2	0.1483	1	0.1483	31.36	0.0008**
Residual	0.0331	7	0.0047		
Lack of fit	0.0331	3	0.011		
Pure error	0	4	0		
Total	1.52	16			

Note: **Highly significant level ($p < 0.01$); *Significant level ($p < 0.05$).

The significance of the regression model was evaluated at the α=0.05 significance level. According to the ANOVA results, the regression model for the seedling extraction success rate has a P-value of less than 0.0001, indicating high statistical significance. Nonsignificant terms were removed, and significant factors were retained.

The regression equations for the response variables Y_1 and Y_2 are expressed as follows.

$$Y_1 = -4.80156 + 4.16074\,X_1 + 0.863394\,X_2 - 13.05821\,X_3 - 0.158211\,X_1X_2 + 0.612083\,X_2X_3 - 0.275933\,X_1^2 - 0.050006\,X_2^2 + 12.18875\,X_3^2 \quad (7)$$

$$Y_2 = 1.11999 - 0.665483X_1 - 1.46383X_2 + 5.67771X_3 + 0.7525X_1X_3 - 0.291583X_2X_3 + 0.018392X_2^2 - 4.69188X_3^2 \quad (8)$$

Optimization of transplanting claw parameters based on the NSGA-II algorithm

Response surface methodology (RSM) evaluates the significance of influencing factors and their interactions through the fitted models obtained in post-processing, thereby identifying optimal solutions. However, in practical applications, the two evaluation indices may influence each other to a certain extent. Therefore, the NSGA-II algorithm (a nondominated sorting genetic algorithm with elitist strategy) was employed to optimize the design parameters of the transplanting claw.

A multi-objective optimization model was constructed in the modeFRONTIER software, as shown in Figure 7. In the figure, X_1 (A), X_2 (B), and X_3 (C) represent the design parameters of the transplanting claw, while obj_1 and obj_2 correspond to the regression equations for stem stress and deformation, respectively. The NSGA-II algorithm was selected in modeFRONTIER, and the control parameters were configured as follows. Mutation probability is 0.1. Crossover probability is 0.9. Population size is 20, and termination generation is 50.

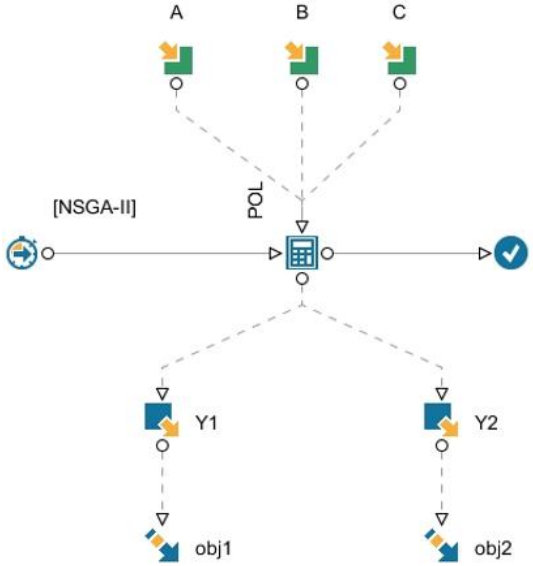

Fig. 7- Optimization model based on modeFRONTIER

Figure 8 shows the bubble chart of the Pareto solution set. The green bubbles represent the overall Pareto solution set, while the bubbles with red edges correspond to the Pareto front solutions. As illustrated in the figure, most design solutions lie along the Pareto front, indicating continuous trade-offs between the two optimization objectives Y_1 and Y_2 . This demonstrates that the NSGA-II algorithm (nondominated sorting genetic algorithm with elitist strategy) achieves favorable optimization performance.

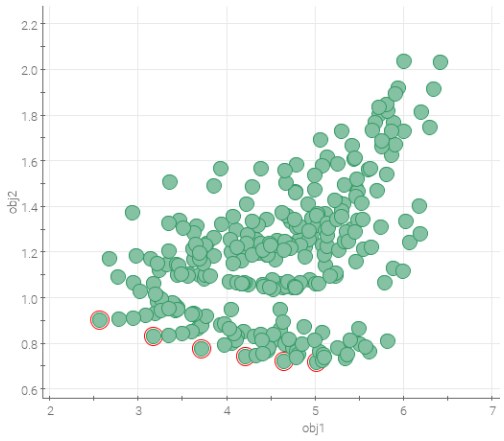

Fig. 8 - Bubble diagram of NSGA-II solution set

Figure 9 presents the parallel coordinates plot based on the Pareto solution set. The horizontal axis represents the design parameters and performance indicators of the transplanting claw, and each solution is visualized as a polyline. The red polylines denote the Pareto front solutions, which represent all feasible optimal solutions.

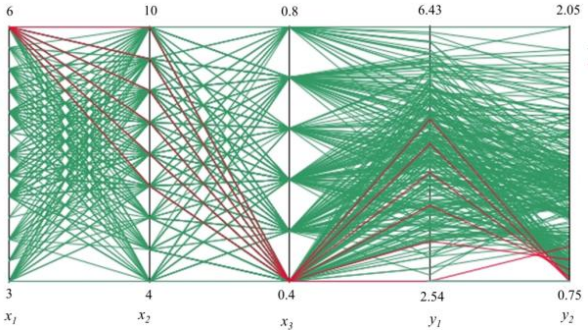

Fig. 9 - Parallel coordinate plot of the NSGA-II solution

Based on the Pareto front solutions, the optimal parameter combination was determined as follows: foam thickness (x_1) is 6 mm, foam width (x_2) is 6.4 mm, and clamping torque (x_3) is 0.4 N·m. The NSGA-II algorithm predicted a stem stress of 3.2 MPa and a stem deformation of 0.8 mm. When the optimized parameters were reintroduced into the simulation model, the resulting stem stress was 3.1893 MPa and the deformation was 0.8024 mm, both of which closely match the predicted values. This confirms the feasibility and effectiveness of using the NSGA-II algorithm for optimizing the transplanting claw design.

CONCLUSIONS

Based on the design of the clamping-type transplanting claw, Box–Behnken simulation experiments combined with the NSGA-II algorithm were used to optimize its key design parameters. The main conclusions are as follows.

(1) Using the Transient Structural module in ANSYS Workbench, a dynamic simulation model of the seedling taking process for the clamping-type transplanting claw was constructed and analyzed in conjunction with a central composite design. Foam thickness, foam width, and clamping torque were selected as the experimental factors, while the stress and deformation at the clamping region of the tomato stem after successful extraction were used as response indices in the Box–Behnken design. Based on the variance analysis and response surface of the regression models, the significance of each factor and their interactions was evaluated, and the corresponding regression equations for the response indices were obtained.

(2) The fitted regression equations were further subjected to multi-objective optimization using the NSGA-II algorithm, yielding the Pareto front of the optimization objectives. An optimal solution from the Pareto front was selected as the design parameter set for the transplanting claw. When the foam thickness is 6 mm, the foam width is 6.4 mm, and the clamping torque is 0.4 N·m, the resulting stem stress is 3.1893 MPa and the stem deformation is 0.8024 mm. These values closely match the predicted results, providing theoretical guidance for the design of the transplanting claw.

(3) Limitations and future work

This study is entirely based on finite element simulations. Experimental validation on a physical prototype is necessary to confirm the optimized parameters and to measure actual stem damage rates. Moreover, the biological damage threshold of tomato stems (e.g., stress or strain at which vascular bundle rupture occurs) was not experimentally determined for the specific cultivar used. Future work will include: (1) Constructing a test rig with real-time force and deformation measurement. (2) Conducting destructive tests to establish a precise failure criterion. (3) Validating the NSGA-II optimization results with physical seedling taking trials. Despite these limitations, the combination of Box-Behnken design and NSGA-II provides a robust framework for transplanting claw optimization.

ACKNOWLEDGEMENT

This work was supported by Key Project in Liaoning Agricultural Vocational and Technical College (LnzkA202504) and Agricultural Science and Technology Talent Project in Department of Agriculture and Rural Affairs of Liaoning Province (XLYC2413011).

REFERENCES

[1] Choi, W. C., Kim, D. C., Ryu, I. H. (2002). Development of a Seedling Pick-Up Device with Optimized Claw for Vegetable Transplanters. *Transactions of the ASAE*, 45(1), 13-19.

[2] Jo, J. S., Okyere, F. G., Kim, H. T. (2018). Improvement of Claw-type Seedling Pick-up Device for a Vegetable Transplanter. *Journal of Biosystems Engineering*, 43(3), 202-210.

[3] Sharma, A., Khar, S. (2022). Current Developments in Transplanting Claw for Vegetable Transplanters in Developing Countries. *International Journal of Vegetable Science*, 28(5), 417-440.

[4] Chen, H. T., Lin, J., Wang, J. W. (2015). Design and Experiment of Seedling Picking Mechanism for Vegetable Transplanters. *Computers and Electronics in Agriculture*, 119, 215-223.

[5] Cui, Q. L., Guo, Y. M., Shi, Y. G. (2017). Kinematic Simulation and Experimental Study of Cam-linkage Seedling Transplanting Claw. *Biosystems Engineering*, 162, 89-101.

[6] Jia, B.Y., Ye, M., Zhai, X.J. (2019). Design and Test of a Cam-linkage Combined Seedling Picking Device for Vegetable Transplanters (凸轮-连杆组合式蔬菜移栽取苗装置的设计与试验). *Applied Engineering in Agriculture*, 35(6), 987-996.

[7] Wen, Y.C., Zhang, J.X., Tian, K.P. (2021). Design and Experiment of a Fully Automatic Seedling Picking Device for Vegetable Plug Seedling Transplanters (蔬菜穴盘苗全自动移栽机取苗装置的设计与试验). *Transactions of the ASABE*, 64(3), 765-774.

[8] Wang, X., Huang, Q., Wu, D., Xie, J., Cao, M. Liu, J. (2025). Predicting Minimum Temperatures of Plastic Greenhouse During Strawberry Growing in Changfeng. A Comparison of Machine Learning Algorithms and Multiple Linear Regression. *Agronomy* 15, 709.

[9] Paradkar, V., Raheman, H., Rahul, K. (2021). Development of a Robotic Arm with Adaptive Claw for Paper Pot Seedling Transplanting. *Artificial Intelligence in Agriculture*, 5(5), 52-63.

[10] Cheng, B., Wu, H., Zhu, H., Liang, J., Miao, Y., Cui, Y., Song, W. (2024). Current status and analysis of key technologies in automatic transplanters for vegetables in China. *Agriculture-Basel*, 14(12), 2168.

[11] Wang, J.W., Li, Z.C., Tang, H.L. (2020). Design of a Flexible Clamping Transplanting Claw and Experiment on Seedling Damage Characteristics. *Agricultural Engineering Research*, 29(2), 100325.

[12] Xin, W., Yang, Z. H., Jin, X. (2023). Design and Experiment of an Adjustable Transplanting End-effector Based on Double Cam Mechanism. *Agriculture*, 13(5), 987.

[13] Yin, J. J., Liu, Y. Q., Xie, Y. (2010). Visual Optimization Design of a Manipulator Claw for Rice Transplanting. *IEEE International Conference on Mechatronics and Automation*, 483-486.

[14] He, T., Li, H., Shi, S. (2023). Adaptability Test of Transplanting Claw for 2ZBX-2A Vegetable Transplanter. *Journal of Applied Sciences*, 23(2), 1092-1101.

[15] Mohith, S., Karanth, P. N., Kulkarni, S.M. (2019). Recent Trends in the Design of Precision Transplanting Claw for Agricultural Machinery. *Mechatronics*, 60, 34-55.

[16] Francesca, D.C., Beniamino, L.M.M. (2019). Effect of Transplanting Claw Structure on Seedling Survival Rate of Faba Bean. *Agriculture*, 9(12), 253.

[17] Chang, J.H., Hu, X. W., Zhang, J. (2021). Design and Performance Test of a Mechanical Seedling Picking System for High-speed Transplanters. *Artificial Intelligence in Agriculture*, 5(2), 64-71.

[18] Kunz, G., Perondi, E., Machado, J. (2018). Design Strategy for Reliable Control of Transplanting Claw Trajectory. *Mechatronics*, 49, 89-98.

[19] Khadatkar, A., Magar, A.P., Sawant, C.P., Modi, R.U. (2024). Development and testing of automatic seedling extractor in robotic transplanter using mechatronics for nursey seedlings. *Discover Applied Sciences*, 6(2), 51.
[20] Daisuke, M., Tohru, Y. (2019). Design of a Low-damage Transplanting Claw for Leafy Vegetable Seedlings. *Agriculture*, 9(11), 230.